Nanoelectronics of a DNA Molecule

E.L. Albuquerque†, U.L. Fulco

Departamento de Biofísica e Farmacologia,
Universidade Federal do Rio Grande do Norte
59072-970, Natal-RN, Brazil
† *eudenilson@gmail.com*

E.W.S. Caetano

Instituto Federal de Educação, Ciência e Tecnologia do Ceará, 60040-531,
Fortaleza-CE, Brazil

V.N. Freire

Departamento de Física, Universidade Federal do Ceará, Campus do Pici, 60455-760,
Fortaleza-CE, Brazil

M.L. Lyra, F.A.B.F. Moura

Instituto de Física, Universidade Federal de Alagoas 57072-970, Maceió, Brazil

1. Introduction

The field of nanotechnology has emerged as one of the most important areas of research in the near future. While scientists have been hardly aspiring to controllably and specifically manipulate structures at the micrometer and nanometer scale, nature has been performing these tasks and assembling structures with great accuracy and high efficiency using specific biological molecules, such as DNA and proteins.[1,2]

As a consequence, there has been a tremendous interest in recent years to develop concepts and approaches for self-assembled systems, searching for their electronic and optical applications.[3] Biology can provide models and mechanisms for advancing this approach, but there is no straightforward way to apply them to electronics since biological molecules are essentially electrically insulating.[4] However, exquisite molecular recognition of various natural biological materials can be used to form a complex network of

potentially useful particles for a variety of optical, electronic, and sensing applications.[5] For instance, investigations of electrical junctions, in which single molecules or small molecular assemblies operate as conductors connecting traditional electrical components, such as metal or semiconductor contacts, constitute a major part of what is nowadays known as molecular electronics.[6–8] Their diversity, versatility, and amenability to control and manipulation, make them potentially important components in nanoelectronic devices.[9]

For physicists, this continuing progress and the consequent need for further size miniaturization, makes the Desoxyribo-Nucleic-Acid (DNA) molecule, the basic building block of living species and carrier responsible of the genetic code,[10] the best candidate to fulfill this place. Arguably, one of the main challenging quest of nowadays science, the human DNA is around 6 mm long, has about 2×10^8 nucleotides and is tightly packed in a volume equal to 500 μm^3.[11] If a set of three nucleotides can be assumed to be analogous to a byte, then these numbers represent either 1 Kb μm^{-1} (linear density) or 1.2 Mb μm^{-3} (volume density), an appreciation of how densely information can be stored in the DNA molecule.

A complete DNA molecule is a chromossome, with protein components present as structural support. The DNA of each gene carries a chemical message which signals to the cell how to assemble the amino acids in the correct sequence to produce the protein for which that gene is responsible. The information is contained in the sequence of the monomers called nucleotides, which make up the DNA molecule, whose structure consists of a base together with a backbone of alternating sugar molecules and phosphate ions. There are four different nucleotides in DNA, differing in the base components, linked together forming a backbone of alternating sugar-phosphate residues with the bases that carries the information of the gene. For practical reason these nucleotides can be considered as a symbolic sequence of a four letter alphabet, namely guanine (G), adenine (A), cytosine (C) and thymine (T).

Numerous algorithms have been introduced to characterize and graphically represent the genetic information stored in the DNA nucleotide sequence. The goal of these methods is to generate representative pattern for certain sequences, or groups of sequences. Notwithstanding, the design of DNA-based devices for molecular nanoelectronics is not yet an easy task since they are crucially dependent upon elucidation of the mechanism and dynamics of electrons and hole transport in them. Besides, unlike proteins, DNA is not primarily an electron/hole-transfer problem, and its suitabil-

ity as a potential building block for molecular devices may not depend only on long-distance transfer of electrons and holes through the molecule. However, the discovery that DNA, like proteins, can conduct an electrical current, has made it an interesting candidate for nanoelectronic devices, which could help to overcome the limitations that classical silicon-based electronics is facing presently. Indeed, individual DNA molecules are very suitable for producing a new range of devices that are much smaller, faster and more energy efficient than the present semiconductor-based ones.[12]

In fact, DNA offers a solution to many of the hurdles that need to be overcome, since it has the capacity of self-assemblage and self-replication, making possible to produce nanostructures with a precision that is not achievable with the classical silicon-based technologies.[13] On the other hand, their conductivity properties are still under intense debate. Controversial reports consider that DNA may be a good linear conductor, while others have found that it is somewhat more effective than proteins, even when the molecules had perfectly ordered base pairs.[14] Recently measurements of electrical transport through individual short DNA molecules indicated that it has a wide-band-gap semiconductor behavior.[15] Besides, strongly deformed DNA molecules deposited on a substrate and connected to metallic electrodes can behave as an insulator or a conductor depending, among other things, on the ratio between the thickness of the substrate and the molecule.[16] On the other hand, it was recently shown, using the density functional theory (DFT) framework, that anhydrous crystals of the DNA bases are wide gap semiconductors.[17] Guanine and cytosine (adenine and thymine) anhydrous crystals were predicted to be a direct (indirect) band gap semiconductors, with energy gap values equal to 2.68 eV and 3.30 eV (2.83 eV and 3.22 eV), respectively, while the experimentally estimated band gaps measured were 3.83 eV and 3.84 eV (3.89 eV and 4.07 eV), in the same order. The obtained electronic effective masses at band extremes showed that, at low temperatures, these anhydrous crystals of DNA bases behave like wide gap semiconductors for electrons moving along the nucleobases stacking direction, while the hole transport are somewhat limited.

These seemingly contradictory theoretical and experimental results are caused mainly by three factors:

(a) native DNA consists of a double helix with an aperiodic sequence, sugar-phosphate side chains, and water as well as ions surrounding it;
(b) the topology of the double-helix, which is not a rigid object, with the different constituents of DNA moving relative to each other;
(c) the works so far have been performed by using quite different theoretical

methods and experimental techniques.

Within the above context, the purpose of this chapter is to present a comprehensive and up-to-date account of the main electronics properties of the DNA molecule within the context of quasiperiodicity of the bases arrangement and the role played by short- and long-range correlation effects, looking for nano-size devices.[18,19] The DNA is usually described as a two-dimensional short-ranged correlated random chain, but nothing prevents that the DNA chain can be grown following quasiperiodic sequences as, for instance, the Fibonacci (FB) and Rudin-Shapiro (RS) ones. These structures exhibit interesting properties, namely:

(a) they have a complex fractal spectra of energy, which can be considered as their indelible mark;
(b) they also exhibit collective properties that are not shared by their constituents.

These collective properties are due to the presence of long-range correlations, which are expected to be reflected somehow in their various spectra (electronic transmission, density of states, etc.) defining another description of disorder (for up to date reviews, see Refs.[20–22]). Besides, the introduction of long range correlations in aperiodic or genomic DNA sequences markedly change their physics and can play a crucial role in their charge transfer efficiency, making a strong impact on their engineering biological processes like gene regulation and cell division.[23,24] Moreover, the nature of this long range correlation has been the subject of intense investigation, whose possible applications on electronic delocalization in the one-dimensional Anderson model have been recently discussed.[25]

It is well known that the DNAs electronic band structure is composed of two main bands of allowed states separated by an energy gap, similar to those of a solid-state semiconductors. At half filling the presence of the energy gap gives to these molecules an intrinsic insulator character. The introduction of defects may generate states within the gap and substantially improve the conductance, specially of finite molecules. In single-strand DNA molecules, defects may be originated within the own nucleotide sequence or by laterally attaching new structures at random.[26] However, disorder modifies profoundly the nature of the electronic states in 1D systems. All states usually become exponentially localized for any amount of disorder. Such exponential localization competes with the above improvement on the conductance associated with the presence of states within the gap. Therefore, schemes for introducing defects that minimize the tendency of

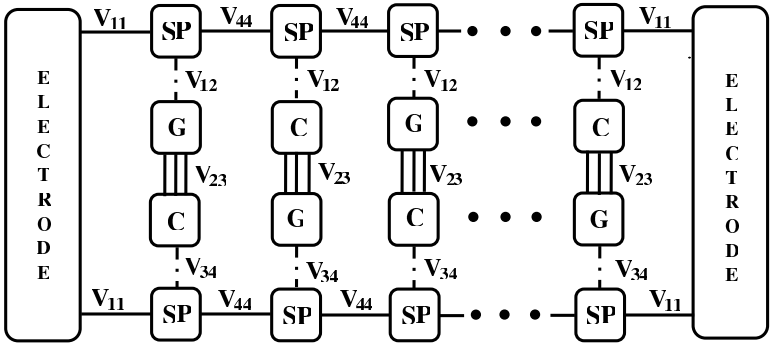

Fig. 1. Schematic representation of a ladder DNA molecule, including the sugar-phosphate contribution.

exponential localization of the electronic states are essential to tailor the electronic transport properties of DNA-based nanoelectronic devices.

We will not consider the possible influence of the environment, although its effects may act as a source of disorder. However we do consider the influence of the sugar-phosphate backbone, since it promotes the emergence of a band gap of the order of the hopping integral.[27] Recent results showed that the hybridization of the overlapping p-orbital in the base-pair stack coupled to the backbone is sufficient to predict the existence of a gap in the nonequilibrium current-voltage characteristics, with a minimal number of parameters.[28]

This work is structured as follows: we present in Section 2 our theoretical model based on an electronic tight-binding Hamiltonian together with a transfer-matrix approach to simplify the algebra, which can be otherwise quite heavy, suitable to describe a finite DNA segment. Section 3 deals with the conductivity of the DNA molecule through their electron transmittance coefficient. Solving numerically a time-dependent Schrödinger equation, we compute also the time dependence of the *spread* of the wave function, as a function of time, for all DNA models considered here. In section 4 we investigate the one-electron states in single-strand binary DNA-based finite segments with diluted base pairing. Considering a framework in which the DNA molecule is sandwiched by two electrodes (donnor-DN and acceptor-AC, respectively), we discuss in section 5 some basic properties of their I-V characteristics curves, following a Landauer-Büttiker formulation. Finally, the conclusions of this work are presented in Section 6.

2. Theoretical Model

Our Hamiltonian is an effective tight-binding model describing one electron moving in a double-strand DNA, including the contribution of the sugar-phosphate (SP) backbone. Considering a localized basis with a single orbital per site and nearest-neighbor interactions, as it is depcticted in Fig. 1, we have:[29]

$$\begin{aligned} H = & \sum_n \Big[\omega_{SP}^n |n,1\rangle\langle n,1| + \omega_\alpha^n |n,2\rangle\langle n,2| + \omega_\beta^n |n,3\rangle\langle n,3| + \omega_{SP}^n |n,4\rangle\langle n,4|\Big] \\ & + \sum_n \Big[V_{12}(\alpha \to SP)[|n,1\rangle\langle n,2| + |n,2\rangle\langle n,1|]\Big] \\ & + \sum_n \Big[V_{23}(\alpha \to \beta)[|n,2\rangle\langle n,3| + |n,3\rangle\langle n,2|]\Big] \\ & + \sum_n \Big[V_{34}(\beta \to SP)[|n,3\rangle\langle n,4| + |n,4\rangle\langle n,3|] + V_{SS}(|n,S\rangle\langle n,S|)\Big] \\ & + \sum_n \Big[V_{11}(SP \to S)(|n,1\rangle\langle n-1,1|) + V_{44}(SP \to SP)(|n,4\rangle\langle n \pm 1,4|)\Big], \end{aligned} \tag{1}$$

where ω_{SP}^n represents the single energy, in units of $\hbar$, at site n of the sugar-phosphate orbital, with ω_α^n ($\alpha = G, C, A$ or T) being the ionization energy of the respective base α. Also $V_{12}(\alpha \to SP)$, $V_{23}(\alpha \to \beta)$ and $V_{34}(\beta \to SP)$ are the inter-chain first-neighbor electronic overlaps (hopping amplitude), with α, $\beta = G, C, A$ or T, while V_{SS} is the hopping term in the substrate. Besides, $V_{11}(SP \to S) = V_S$ and $V_{44}(SP \to SP) = V_{SP}$ are the intra-chain hopping amplitudes. Here the letter S means the substrate (which here will be considered as a platinum electrode), while SP means the sugar-phosphate backbone.

The Dyson equation is

$$G(\omega) = \omega^{-1}[I + HG(\omega)], \tag{2}$$

where I is the identity matrix and H is the Hamiltonian given by (1). Within this framework, the electronic density of state (DOS) follows:

$$\rho(\omega) = -(1/\pi)\mathrm{Im}[Tr\langle n|G(\omega)|n\rangle], \tag{3}$$

where Im means the imaginary part of the argument shown between brackets. The energies $\omega_{\alpha,\beta}$ are chosen from the ionization potential of the respective bases, i.e., $\omega_G = 7.77, \omega_C = 8.87, \omega_A = 8.25$, and $\omega_T = 9.13$,

all units in eV, representing the guanine (G), cytosine (C), adenine (A), and thymine (T) molecules, respectively.[30–32] Also, we use the energy of the platinum electrode $\omega_S = 5.36$ eV, which is related to the work function of this metal,[33] while the energy of the sugar-phosphate backbone is $\omega_{SP} = 12.27$ eV.[34] The hopping between the base pair is $V_{23}(\alpha \to \beta) = 0.90$ eV.[34] The potential at the interface DNA-substrate (platinum) is considered to be the difference between the Fermi's level of the platinum and the HOMO's (Highest Occupied Molecular Orbital) of the sugar-phosphate, giving us $V_S = 6.91$ eV.[34] The hopping potentials between the base and the sugar-phosphate (SP) backbone is $V_{12}(\alpha \to SP) = V_{34}(\alpha \to SP) = 1.5$ eV, while in the substrate (a platinum electrode) is $V_{SS} = 12$ eV.[35] Finally, the hopping potential between the sugar-phosphate backbone, is $V_{SP} = 0.02$ eV.[36]

For the DNA sequence of the first sequenced human chromosome 22 (Ch 22), entitled NT_{011520}, the number of letters of this sequence is about 3.4×10^6 nucleotides.[37] This sequence was retrieved from the internet page of the National Center of Biotechnology Information. We will consider finite segments of CH22 chromosome starting at the 1500-th nucleotide.

To setup a quasiperiodic chain of Rudin-Shapiro type, we consider the nucleotide G (guanine) as seed. The sequence can then be built through the inflation rules $G \to GC$, $C \to GA$, $A \to TC$, and $T \to TA$. The RS sequence belongs to the family of the so-called substitutional sequences, which are characterized by the nature of their Fourier spectrum. It exhibits an absolutely continuous Fourier measure, a property which it shares with the random sequence.[38] It should be contrasted with the Fibonacci sequence (another substitutional sequence) which displays a dense pure point Fourier measure, characteristic of a true quasicrystal-like structure (for a review of the physical properties of these and others quasiperiodic structures see Ref.[39]). This important difference has been discussed in the literature in connection with the localization properties of both elementary excitations[40] and classical waves[41] in the RS sequence, as compared to other substitutional sequence.

Fig. 2 shows the DOS for several intra-strand nucleobases couplings and for several inter-strands ones, taking into account the three different sequences discussed in this paper: (a) Fibonacci (b) Rudin-Shapiro and (c) human chromosome 22 (Ch 22).[42] Rather than traces of bands, the DOS profile for each structure is fragmented, showing a number of discrete strongly localized bunches of states that are believed to reflect their 1D band structure. Observe that the number of van Hove singularities is big-

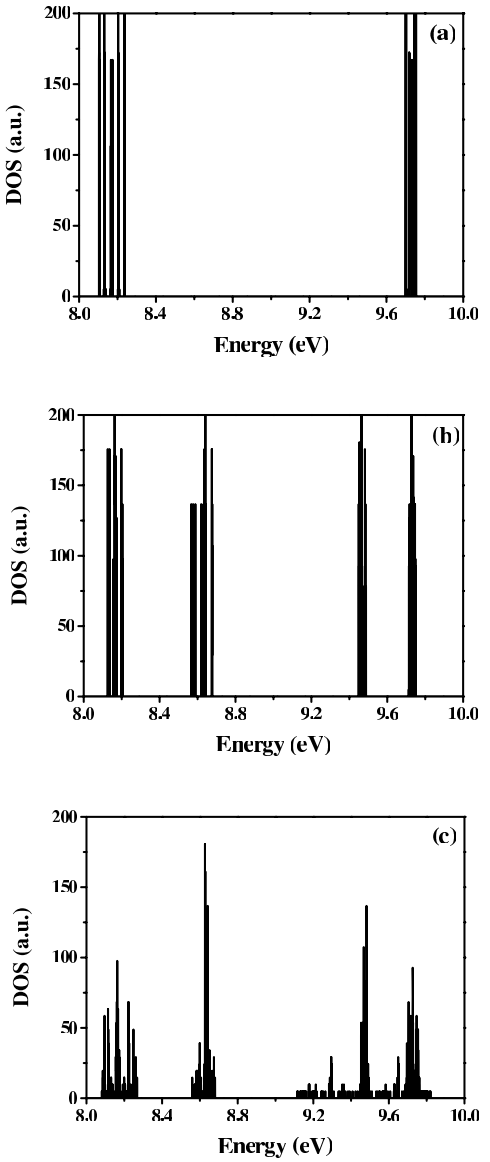

Fig. 2. The eletronic density of states (DOS) in arbitrary units plotted against the energy E (in eV) for: (a) Fibonacci sequence; (b) Rudin-Shapiro sequence; (c) DNA human chromosome 22 (Ch22).

ger for the RS and Ch22 structures than for the simplest Fibonacci one. Indeed, by inspecting Fig. 2, one can observe that for the Fibonacci case, there are two well defined regions around $\omega_G = 7.77$ eV and $\omega_C = 8.87$ eV, respectively. On the other hand, the Rudin-Shapiro and Ch22 structures have four regions centered roughly at the ionization energies of their nucleotides.

3. Conductivity and Wave Packet Dynamics

Consider now that the above sequences are further assumed to be connected to two semi-infinite electrodes whose energies ϵ_m are adjusted to simulate a resonance with the guanine highest occupied molecular orbital (G-HOMO) energy level, i.e., $\epsilon_m = \epsilon_G$. The hopping integrals are chosen such that V_{23}, based on *ab initio* calculations, suggesting the hopping terms in the range 0.1 to 0.4 eV. For this system, the transmission coefficient $T_N(E)$, that gives the transmission rate through the chain and is related with the Landauer resistance, is defined by:[43]

$$T_N(E) = \frac{4 - X^2(E)}{\left[\begin{array}{c} -X^2(E)(\mathcal{P}_{12}\mathcal{P}_{21} + 1) + X(E)(\mathcal{P}_{11} - \mathcal{P}_{22})(\mathcal{P}_{12} - \mathcal{P}_{21}) \\ + \sum_{i,j=1,2} \mathcal{P}_{ij}^2 + 2 \end{array}\right]}, \quad (4)$$

where $X(E) = (E - \omega_m)/V_{23}$, and $\mathcal{P}_{ij}$ are elements of the transfer-matrix $\mathcal{P}$ (see Ref.[43]). For a given energy E, $T_N(E)$ measures the level of backscattering events in the electrons (or hole) transport through the chain.

In Fig. 3 we plot the transmission coefficient $T_N(E)$, as given by Eq. (4), as a function of the energy, in units of eV. We have considered the Fibonacci sequence (Fig. 3a, with generation number $N_F = 12$, corresponding to $n_F = 233$ nucleotides), the Rudin-Shapiro one (Fig. 3b, with generation number $N_{RS} = 7$, corresponding to $n_{RS} = 64$ nucleotides), the random case (Fig. 3c, with $n_{RD} = 64$ nucleotides), and the human chromosome Ch22 (Fig. 3d, with $n_{Ch_{22}} = 64$ nucleotides), respectively. Observe that the transmission bands in all cases are fragmented, which is related to the localized nature of the electron's eigenstates in disordered chains, and reflects the number of passbands in each structure (when the localization factor is zero, the corresponding frequency intervals are known as passbands). It is relevant to stress that the presence of long-range correlations in the disorder distribution is a possible mechanism to induce delocalization in low dimensional systems.[44] However, the actual correlations in our model (hopping mechanism) are not strong enough to produce this correlation-induced

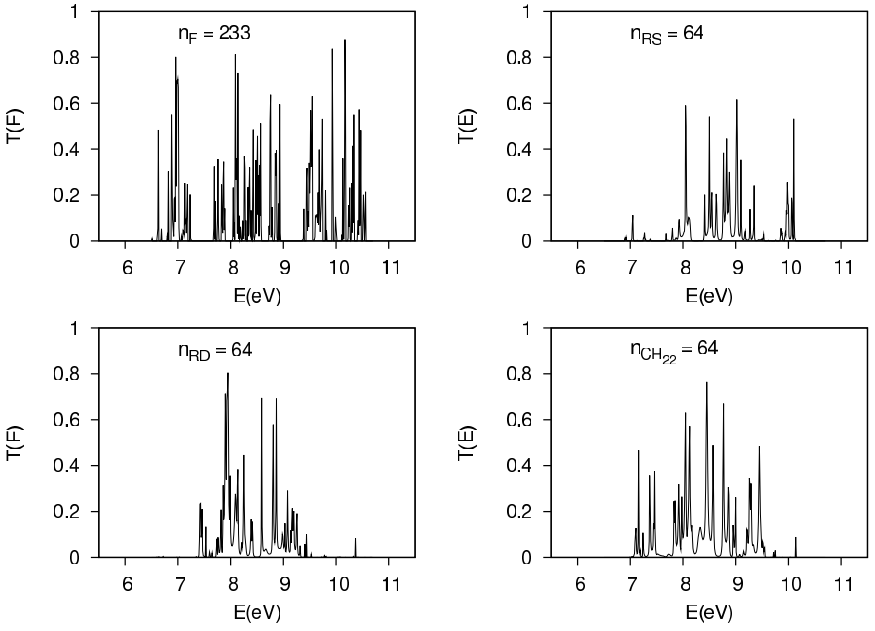

Fig. 3. Transmittance coefficient $T_N(E)$ as a function of the energy E, in units of eV, for: (a) the Fibonacci sequence, with generation number $N_F = 12$, corresponding to $n_F = 233$ nucleotides; (b) the Rudin-Shapiro structure, with generation number $N_{RS} = 7$, corresponding to $n_{RS} = 64$ nucleotides; the random case, with $n_{RD} = 64$ nucleotides; (d) the human chromosome Ch22, with $n_{Ch_{22}} = 64$ nucleotides. Notice that the presence of correlations contributes to the survival of resonant transmission peaks for sequences up to hundreds of nucleotides.

transition, and the stationary states remain all localized. Moreover, the presence of long-range correlations enhances the localization length and, therefore, transmission resonances survive in larger segments as compared with a non-correlated random sequence (see, for instance, the Fibonacci case). Observe also that the transmission coefficient for long-range correlated Rudin-Shapiro sequences, depicts a trend similar to the one produced by the genomic Ch22 sequence.

Focusing now on the wave packet dynamics in the above finite segments, we solved numerically the time-dependent Schrödinger equation and computed the time dependence of the *spread* of the wave function (square root of the mean squared displacement), as a function of time, by using

$$\sigma(t) = \sqrt{\sum_{n=1}^{N} \left[n - \langle n(t)\rangle\right]^2 \, |\psi_n(t)|^2}. \tag{5}$$

The problem involving the spread of one electron wave-functions in low-dimensional disordered systems is a well known issue with several connections with transport properties.[45] In general lines, the wave function of an electron moving in a perfectly periodic potential spreads linearly in time. In the presence of uncorrelated disorder, the scaling theory predicts the absence of extended eigenstates[46] in one-dimensional (1D) systems. Therefore, the width of the time-dependent wave-function saturates in the long time limit, i.e., the electron wave-function remains localized in a finite region around the initial position. The scaling theory prediction of exponential localization of all one-electron eigenfunctions in 1D systems can be violated when special short-range[47] or long-range[48] correlations are present in the disorder distribution. The influence of scale-free disorder in the 3D Anderson transition has also been recently addressed.[49] In particular, the presence of dimer-like correlations on a N-site binary chain produces $\sqrt{N}$ extended states. These states have random phase changes when crossing the dimer impurities which results in a finite coherence length. If the energy of the resonant extended state is within the band of the allowed states of the underlying pure chain, the electron wave-packet experiences a super-diffusive spread.

To study the spread of one-electron wave function, we start from a wave-packet localized at the guanine G site closer to the center of the single- and double-strand segments. In order to avoid finite-size effects, we used larger segments with $N = 1500$. For the Ch22, pair-correlated (PC) and random sequences, an average over 20 distinct segments was employed, to account for configurational variability. Typical results are depicted in Fig. 4. For the wave-packet spread over a single-strand sequence (see Fig. 4a), the long-range correlations in the RS sequence results in a wave-packet spread over a segment which overpass the one achieved in the Ch22 strand by a factor of the order of 1.5. On the other hand, the spread in a completely uncorrelated sequence is just half of that in Ch22, pointing to the importance of the nucleotide correlations. The fact that the spread in the PC sequence is already 3/4 of the spread in the natural Ch22 sequence led to the conjecture that the systematic inclusion of further short-range correlations might be enough to capture the correct one-electron dynamics in DNA molecules.[50]

The above trend concerning the role played by short- and long-range cor-

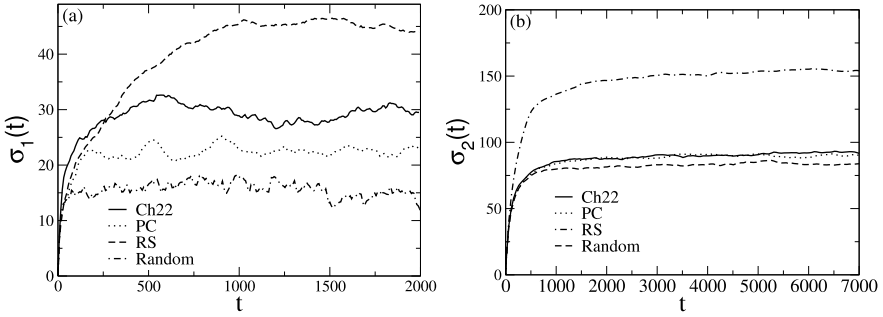

Fig. 4. (a) Spread of the wave function, defined by the time-dependent square root of the mean-square displacement, as a function of time (t) for several kinds of single-strand sequences. (b) The wave-packet spread in double-strand sequences. The long-range correlations in the RS sequence induces a large wave-function spread as compared to the Ch22 sequence. Short-range correlation of the random sequence matches nicely those of the Ch22 human chromosome. Error bars at the long time-regime are of the order of three base pairs.

relations is further strengthened when we analyze the wave-packet spread in double-strand sequences, as shown in Fig. 4b. In this case, the spread in the long-range correlated RS sequences becomes much larger when compared to the single-strand one. This fact is associated to the larger values achieved by the localization length of stationary states, as previously discussed. When compared to the spread in double-strand Ch22 sequences, the RS one allows for the wave-packet spread over a segment which is twice as large due to the excess of correlations. The coupling between strands in Ch22 favored the electron spread which now reaches a segment almost three times larger than in the single-strand sequences. It is instructive to notice that the spread in an uncorrelated double-strand sequence is already close to that in the Ch22, and the inclusion of first neighbors correlations suffices to achieve the same wave-packet spread in Ch22. The above results indicate that long-range correlations are not relevant for the one-electron dynamics in DNA, and that the inclusion of just first-neighbors correlations may be enough to have a quantitative description of the wave-packet spread in double-strand sequences.[51]

4. DNA finite segments with diluted base-pairing

We now present a numerical investigation of the one-electron states in single-strand binary DNA-based finite segments with diluted base pairing. Our opting to consider single-strand molecules was mainly motivated by the

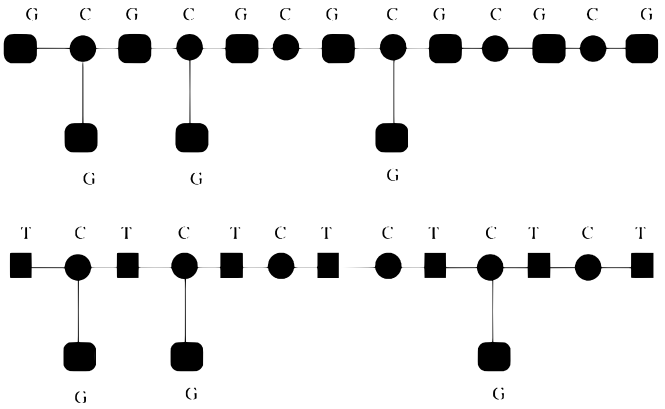

Fig. 5. Schematic representation of the single-strand DNA molecule showing the main periodic chains of alternate bases (CG and CT sequences) with diluted base pairing. Guanine (G) bases are laterally attached at random to a fraction p of the cytosine (C) sites.

fact that these are known to be poorer conductors than the more sophisticated model studied in the previous sections. It was not motivated by the simplicity of the numerical and mathematical treatment, making use, for example, of a renormalization scheme as in Ref.,[52] since similar techniques can be used in either case.

Our main intention was to reinforce that the resonance mechanism reported in our paper leads to an anomalous wave-packet dynamics, even in the worse case of strong localization in single-strand molecules. Specifically, we will consider poly(CG) and poly(CT) segments, at which guanine bases (G) are attached laterally at a fraction of the cytosine (C) bases. Within a tight-binding description, we will compute the density of states and eigenfunctions of the one-electron states. We will show that the model Hamiltonian for this system can be mapped onto that of the Anderson chain with diluted disorder, exploring the influence of the effective disorder on the nature of the one-electron states as well as on the wave-packet dynamics. In particular, we will show that in segments formed with complementary units [as in poly(CG)], base pairing dilution indeed leads to a complete exponential localization of all one-electron states. On the other hand, in chains with non-complementary units [as in poly(CT)], a resonant state is not affected by the disorder and remains extended. In the presence of such resonant state, the wave-packet develops a diffusive dynamics.

In what follows, we will work within a tight-binding approach, whose Hamiltonian describes one electron moving in a geometry composed of a periodic chain of alternate bases (CG or CT sequences). Our model Hamiltonian is constructed considering only the essential ingredients responsible for the quite distinct electronic transport properties of the poly(CG) and poly(CT) molecules with diluted base pairing. We are aware that more realistic models for DNA based molecules shall include other contributions, although these additional terms shall play a similar role in both poly(CG) and poly(CT) molecules.

In the tight-binding Hamiltonian model of electronic transport, the main information taken from the underlying complex structure is the HOMO level of its building blocks and the transfer integrals. However, this is a general feature of single state tight-binding modeling and not a specific aspect of our present model. Furthermore, we would like to stress that previous tight-binding studies have correctly captured several features of the electronic transport of DNA based molecules (for a review see Ref.[53]).

We assume that G bases are laterally attached to the C sites at random, with probability p (see Fig. 5). We consider just a single orbital per site and nearest-neighbor transfer integrals V (along the main chain) and V' (among paired bases). The corresponding time-independent Schrödinger equation for a poly(CG) sequence is given by:[54]

$$E\psi_j^G = V(\psi_{j-1}^C + \psi_{j+1}^C) + \omega_G \psi_j^G \quad \text{for odd j,} \tag{6}$$

$$E\psi_j^C = V(\psi_{j-1}^G + \psi_{j+1}^G) + V'\beta_j \psi_j^G + \omega_C \psi_j^C, \quad \text{for even j.} \tag{7}$$

For a poly(CT) sequence one just has to replace G by T. Here, ω_α ($\alpha = G, T$ or C) represents the on-site potential at the bases G, T or C and ψ_j^α is the wave-function coefficient in the single orbital basis, defined by

$$|\Psi\rangle = \sum_{(j,\alpha)} \psi_j^\alpha |j, \alpha\rangle, \tag{8}$$

where (j, α) runs over all base units. Also, $\beta_j = 1$ with probability p and $\beta_j = 0$ with probability $1 - p$, where p is the concentration of G sites attached to the single stranded main periodic chain. At the sites where $\beta_j = 1$, we have an additional equation:

$$E\psi_j^G = V'\psi_j^C + \omega_G \psi_j^G, \quad \text{for even j and } \beta_j = 1. \tag{9}$$

A clear picture of the nature of the electronic states on the above model can be achieved by performing a decimation procedure of the attached base units. The above tight-binding model for a DNA-based molecule can be mapped onto an effective one-dimensional diluted Anderson model.[55–58] Such model contains a diagonal disorder diluted by an underlying periodicity. The resulting sequence is composed of two inter-penetrating sublattices, one composed of random potentials (Anderson chain), while the other has non-random segments.

The degrees of freedom associated with the lateral DNA bases appearing in the above equations can be removed by substituting[59]

$$\psi_j^G = [V'/(E - \omega_G)]\psi_j^C, \text{ for even j}, \tag{10}$$

into the equation for the coefficients ψ_j^C, yielding:

$$E\psi_j^C = \omega_C^* \psi_j^C + V(\psi_{j-1}^G + \psi_{n+1}^G), \tag{11}$$

where

$$\epsilon_C^* = \omega_C + [V'^2/(E - \epsilon_G)] \tag{12}$$

is the renormalized potential at the cytosine sites at which the G bases are laterally attached. For those cytosine bases with no lateral attachment, the potential remains the bare one.

Therefore, after having eliminated the coefficients associated with the lateral G bases, the remaining set of equations expresses an alternate sequence of CG (or CT). Most importantly, the C sites have now two possible values for the on-site potential, namely ω_C^* with probability p or ω_C with probability $1 - p$, respectively. The remaining bases of the periodic sequence have all the same potential: ϵ_G for poly(CG) or ω_T for poly(CT). The random character of the diluted base-pairing is reflected in a random sequence for the effective on-site energies of the cytosine sites. This kind of sequence is similar to the structure so-called diluted Anderson model. It consists of two inter-penetrating sequences: a periodic sequence containing the guanine or thymine sites, for poly(CG) or poly(CT) respectively, and a random sequence containing bare and renormalized cytosine sites. Due to the periodicity of the non-random sub-lattice, a special resonance energy E_0 appears with vanishing wave-function amplitudes on the random sub-lattice. Therefore, this mode is mainly insensitive to the presence of disorder and may lead to a possible mechanism to induce conductance in such DNA-based molecules.

For the poly(CT) molecule, the resonance energy is $E_0 = \omega_T$. At this energy, the renormalized cytosine potential remains finite, and a divergence of the localization length of the one-electron eigenmodes, as the resonance energy is approach, can be anticipated.[55,57] On the other hand, the resonance energy for poly(CG) molecules is $E_0 = \omega_G$. At this energy, the renormalized cytosine potential diverges. This case corresponds to an effectively infinite disorder which counteracts the delocalization effect. Within such reasoning, one expects diluted base-pairing to induce a stronger localization of the one-electron eigenfunctions in poly(CG) than in poly(CT) chains.

Using a recursion method we can now obtain the electronic density of states (DOS), which is depicted in Fig. 6a,b for three representative values of the concentration of paired cytosine bases, namely:

(i) $p = 0$, corresponding to pure poly(CG) and poly(CT) chains;
(ii) $p = 1$, describing the poly(CG) and poly(CT) chains with guanine bases laterally attached to all cytosine bases;
(iii) $p = 0.5$ representing a typical sequence of diluted base-pairing.

In Fig. 6(a) we display our results for the poly(CG) sequences. As one can see, the electronic density of states has two main bands, which is typical of binary sequences, with the gap for $p = 1$ being larger than for $p = 0$. Such enhancement of the energy gap is a direct consequence of the base-pairing. For $p = 0.5$ one notices that all van Hove singularities at the band edges are rounded off by the presence of disorder. The fluctuations in the DOS have been exploited in the literature to identify the nature of the states.[60,61] The variance in the number of states in a given energy window shall scale linearly with the system size for localized states, while having just a slow logarithmic scaling for extended states. These two regimes reflect the distinct level spacing statistics of localized and extended states. As a result, much smaller fluctuations are attained in the normalized DOS when extended states are present as compared to the fluctuations observed in the energy range corresponding to localized states. These fluctuations are of the same magnitude in both bands, which indicate that these bands are equally affected by disorder.

The DOS for poly(CT)-based chains are depicted in Fig. 6(b). For these molecules, one can observe a series of relevant features not found in the previous case. Firstly, one sees that the two band structure of the binary $p = 0$ case evolves to a three band structure at $p = 1$, as expected for a periodic structure with three distinct sites in the unit cell. It is important

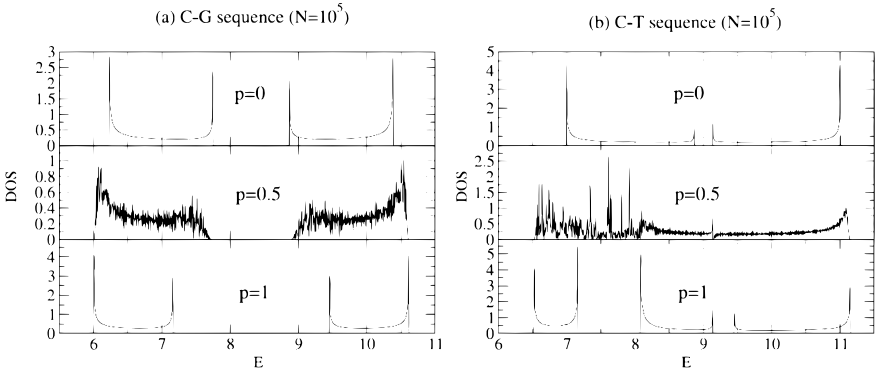

Fig. 6. Plot of the electronic density of states (DOS) versus the reduced energy E/V. (a) Poly(CG)-based DNA sequences. The band gap persists for poly(CG) chains with diluted base-pairing and all van Hove singularities are rounded off; (b) Poly(CT)-based DNA sequences. The bands coalesce for base-pair diluted poly(CT) before splitting into three bands. Disorder does not affect the van Hove singularity at $E = \omega_T$. The gap-less band structure, together with the non-localization of the resonance state, favors the electronic transport in this case.

to stress that, although after renormalization the poly(CT) has just two sites per unit cell at $p = 1$, the energy dependence of the renormalized cytosine potential takes into account the original three-site structure. It is interesting to notice that the bottom of the upper band at $p = 0$ coincides with the top of the middle band at $p = 1$. This energy corresponds exactly to $E_0 = \epsilon_T$. When the concentration of the attached guanine bases increases, the two-band structure firstly coalesces in a single band, before splitting in three bands, as shown for the particular case $p = 0.5$. Further, the van Hove singularities are rounded off, except the one located at E_0 which corresponds to the resonance state insensitive to disorder. Therefore, diluted base-pairing produces a gap-less band structure while keeping the states around E_0 extended, an ideal scenario for electronic transport. Additionally, the DOS exhibits stronger fluctuations at the bottom than at the top of the energy band, pointing that the low-energy states are more strongly localized than the high-energy states.

5. Current-voltage characteristics

The transmission coefficient is a useful quantity to describe the transport efficiency in quantum systems. Nonetheless, $T_N(E)$ is usually difficult to be directly measured experimentally. Notwithstanding, access to transmission

properties can be performed by measuring their I-V characteristics profiles, being aware however, that the application of a voltage bias in the conducting leads (donor-DN and acceptor-AC electrodes) contacting the DNA segment has also some influence on the scattering properties inside the molecule, and direct information on intrinsic effects of sequences on transmission should thus be considered with care.

Taking into account the effective tight-binding Hamiltonian given above (Eq. 1), one can evaluate the I-V characteristics curves by applying the Landauer-Büttiker formulation:[62,63]

$$I(V) = \frac{2e}{h} \int_{-\infty}^{+\infty} T_N(E)[f_{DN}(E) - f_{AC}(E)]dE, \tag{13}$$

where $f_{DN(AC)}$ is the Fermi-Dirac distribution

$$f_{DN(AC)} = \Big[\exp[(E - \mu_{DN(AC)})/k_B T] + 1 \Big]^{-1}. \tag{14}$$

Also, $\mu_{DN(AC)}$ is the electrochemical potential of the two leads (donor-DN and acceptor-AC) fixed by the applied bias voltage V as[64]

$$|\mu_{DN} - \mu_{AC}| = eV. \tag{15}$$

We are assuming the Fermi level energy equal to zero. The current onset is crucially dependent on the electrochemical potentials of the leads that can be altered by the coupling to molecules, which is another important issue to be separetely considered. For simplicity, before bias voltage is applied, the electrochemical potential of the whole system is taken to be zero. It is important to emphasize that the transmittance $T_N(E)$ should be calculated also for negative values of energy.

Current-voltage characteristics of double-strand DNA sequences are plotted in Fig. 7 for Fibonacci (Fig. 7a), Rudin-Shapiro (Fig. 7b), the random case (Fig. 7c) and the human chromosome Ch22 (Fig. 7d), respectively.[65] We are assuming a linear voltage drop across the DNA molecules by means of the usual expression, numerically computed near zero temperature, as given by Eq. (13). To reproduce the potential mismatch at zero bias, the energy difference between the guanine HOMO energy level and the metallic Fermi level of the electrode is set to 1.2 eV.[66] As the voltage drop is switched on, the transmission coefficient $T_N(E)$ becomes voltage-dependent, resulting in transmission band shifts (shown in Fig. 7 for all cases studied here), which in turn lead to a voltage threshold modulation.

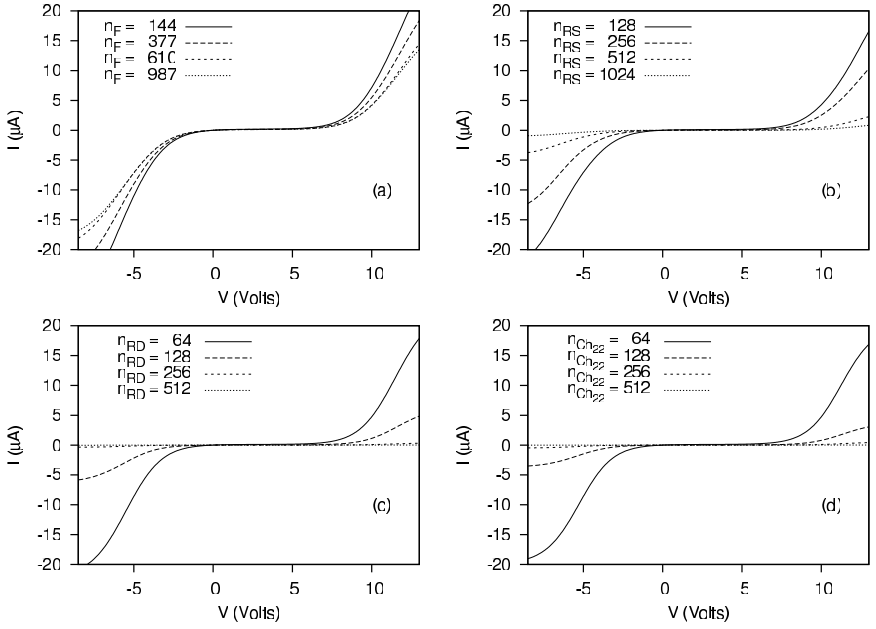

Fig. 7. Current-voltage characteristics of double-strand DNA sequences for (a) Fibonacci; (b) Rudin-Shapiro; (c) the random case; (d) the human chromosome Ch22, respectively.

To extract the main features of tunneling currents in DNA chains, let us compare the behavior of the genomic Ch22 (Fig. 7d) with those characterizing the quasiperiodic and random structures (Figs. 7a,b,c) under the resonance condition given by the hopping term choice V_{23}= 1 eV. In this case, if the potential barrier between the metallic contacts and the DNA is set to zero, a staircase in the plot I-V is found.[67]

As soon as a potential barrier between the DNA and the metals is introduced (1.2 eV), the I-V characteristic curves show the profiles depicted in Fig. 7. The current threshold at a given voltage scale is not sensitive concerning the different structures considered here, mainly due to the electronic correlations presented by the structures. However, such correlations shall depend strongly on the intra-chain coupling, and further studies considering more realistic model parameters would be needed in order to infer about the actual relevance of this treshold enhancement in DNA molecules. Observe the striking agreement between the I-V characteristic curves for the random and the genomic Ch22 case. Such agreement can be accounted by

the short-range pair correlations shared by them, suggesting that the inclusion of just first-neighbors intra-strand pair correlations on the nucleotide distribution can provide an adequate description of the DNA electronic properties.

6. Conclusions

Over the past few years, bionanomaterial science has emerged as a new exciting field in which theoretical and experimental studies of nanobiostructures have stimulating a broader interest in developing the field of nanometer-scale electronic devices. In particular, intelligent composite biological materials have become a new interdisciplinary frontier in life science and material science. Nevertheless, the construction of nanometer-scale circuits remains problematic, and the use of molecular recognition processes and the self-assembly of molecules into supramolecular structures might help overcome these difficulties. In this context, the ability to choose the sequence of nucleotides, and hence provide the addressability during the self-assembly processes, besides its inherent molecular recognition, makes DNA an ideal molecule for these applications.

Aiming to further contribute to the present understanding of the role played by correlations on the electronic properties of DNA segments, we have studied here the electronic transport properties of finite sequences of nucleotides within a tight binding approach of DNA sequences with pure diagonal correlated disorder. In order to unreveal the actual relevance of short and long range correlations, we compared the transmission spectra and the wave packet spread on segments of the Ch22 human chromosome with those resulting from the quasi-periodic (RS and FB) and randomic structures. We obtained that the long-range correlations present in Ch22 and RS sequences are responsible for the slow vanishing of some transmission peaks as the segment size is increased, which may promote an effective electronic transport at specific resonant energies of finite DNA segments. On the other hand, much of the anomalous spread of an initially localized electron wave packet can be accounted by short-range pair correlations on DNA. This finding suggests that a systematic approach based on the inclusion of further short-range correlations on the nucleotide distribution can provide an adequate description of the electronic properties of DNA segments.

We also investigated the nature of the one-electron eigenstates within a tight-binding model of DNA-based poly(CG) and poly(CT) molecules with diluted base-pairing. The model considers that guanine nucelotides

are allowed to attach laterally to the cytosine bases of the main chain with probability p. We demonstrated that this model can be exactly mapped on the diluted Anderson model, consisting of two inter-penetrating chains. One of these chains is composed by non-random units: guanine (G) sites for poly(CG) or thymine (T) sites for poly(CT). The second chain is a random sequence of bare cytosine sites with on-site potential ϵ_C and renormalized cytosine sites with effective on-site potential.

Solving the time-dependent Schrödinger equation to follow the time-evolution of an initially localized wave-packet, we found qualitatively distinct influences of diluted base-pairing in each chain model. For the poly(CG) case, the disorder introduced by the diluted base-pairing promotes the exponential localization of all one-electron states. Furthermore, it enhances the gap between the two main bands of allowed energy states. These two factors reinforces the insulator character of this molecule. On the other hand, for poly(CT) molecules, there is a resonant mode with energy $E_0 = \omega_T$ which is not affected by the disorder and remains extended with a Bloch-like character. Besides, the two energy bands, typical of the pure poly(CT) molecule, coalesce in a single band for intermediate dilution before splitting in three bands. Therefore, when the Fermi energy coincides with the resonance energy, we have a typical scenario favoring electronic transport: a gap-less density of states with extended states near the Fermi level. As one approaches the resonance energy from below, the localization length of the one-electron modes diverges. Above E_0 the localization length remains finite. This feature implies that hole transport shall be predominant over electron transport.

Regarding the I-V characteristic curve, it seems to be accounted by the short-range pair correlations, suggesting that the inclusion of just first-neighbors intra-strand pair correlations on the nucleotide distribution provides an adequate description of the DNA's electronic properties. However, as the electron transmissivity depends strongly on the intra-chain coupling, further studies considering more realistic model parameters would be needed in order to infer about the actual relevance of this behavior in DNA molecules.

These latest developments have provided the motivation and focus for the proposed review article. Due to the potential device applications of such systems, our intention here was to provide a review text with up to date information about the DNA's unique physical properties, as highlighted above. This includes experimental techniques of interest to experimentalists, keeping in mind that, since experimental reality is approaching the-

oretical models and assumptions, detailed analysis and precise predictions are being made possible nowadays.[68–71]

Acknowledgements

We would like to congratulate again Gene and Liacir for their 70 years. This work was partially financed by the Brazilian Research Agencies CAPES (PNPD, Procad and Rede NanoBioTec) and CNPq (INCT-Nano(Bio)Simes, FAPERN/CNPq/Pronex and Procad-Casadinho).

References

1. S. Luryi, J.-M. Xu and A. Zaslavsky (eds.), *Future Trends in Microelectronics: the Road Ahead* (Wiley, New York, 1999).
2. R. G. Endres, D. L. Cox and R. R. P. Singh, *Rev. Mod. Phys.* **76**, 195 (2004).
3. S. Datta (ed.), *Quantum Transport: Atom to Transistor* (Cambridge University Press, New York, 2005).
4. E. Braun and K. Keren, *Adv. Phys.* **53**, 441 (2004).
5. C. Nicoloni (ed.), *Molecular Bioelectronics* (World Scientific, Singapore, 1996).
6. G. Cuniberti, G. Fagas and G. Richter (eds.), *Introducing Molecular Electronics* (Lecture Notes in Physics) (Springer, Berlin, 2005), vol. 680.
7. E. Braun, Y. Eichen, U. Sivan and G. Ben-Yoseph, *Nature* **391**, 775 (1998); S. O. Kelley and J. K. Barton, *Science* **283**, 375 (1999); L. T. Cai, H. Tabata and T. Kawai, *Appl. Phys. Lett.* **77**, 3105 (2000); A. Y. Kasumov *et al.*, *Science* **291**, 280 (2001); K. W. Hipps, *Science* **294**, 536 (2001).
8. M. Taniguchi and T. Kawai, *Phys. Rev. E* **70**, 11913 (2004); C. Joachim and M. A. Ratner, *Proc. Natl. Acad. Sci. USA* **102**, 8801 (2005).
9. J. Park *et al.*, *Nature* **417**, 722 (2002); W. J. Liang, M. P. Shores, M. Bockrath, J. R. Long and H. Park, *Nature* **417**, 725 (2002).
10. J. D. H. Watson and F. H. C. Crick, *Nature* **171**, 737 (1953); *Nature* **171**, 964 (1953); F. H. C. Crick and J. D. H. Watson, *Proc. R. Soc. Lond.* **223**, 80 (1954).
11. H. Lodish, D. Baltimore, A. Berk, S. L. Zipursky, P. Matsudaira and J. Darnell (eds.), *Molecular Cell Biology* (Scientific American Books Inc., New York, 1995).
12. H.-A. Wagenknecht (ed.), *Charge Transfer in DNA: From Mechanism to Application* (Wiley, New York, 2005).
13. F. D. Lewis *et al.*, *Science* **277**, 673 (1997); K. Keren, R. S. Berman, E. Buchstab, U. Sivan and E. Braun, *Science* **302**, 1380 (2003); Y. Zhang, R. H. Austin, J. Raeft, E. C. Cox and N. P. Ong, *Phys. Rev. Lett.* **89**, 198102 (2002).
14. E. Winfree, F. Liu, L. A. Wenzler and N. C. Seeman, *Nature* **394**, 539 (1998).
15. D. Porath, A. Bezryadin, S. De Vries and C. Dekker, *Nature* **403**, 635 (2000); B. Xu, P. Zhang, X. Li and N. Tao, *Nano Lett.* **4**, 1105 (2004).

16. A. Yu. Kasumov, D. V. Klinov, P.-E. Roche, S. Guéron and H. Bouchiat, *Appl. Phys. Lett.* **84**, 1007 (2004).
17. F. F. Maia Jr., V. N. Freire, E. W. S. Caetano, D. L. Azevedo, F. A. M. Sales and E. L. Albuquerque, *J. Chem. Phys.* **134**, 175101 (2011).
18. E. Shapir *et al.*, *Nature Mater.* **7**, 68 (2008).
19. A. Malishev, *Phys. Rev. Lett.* **98**, 096801 (2007).
20. E. L. Albuquerque and M. G. Cottam, *Phys. Rep.* **233**, 67 (1993).
21. E. L. Albuquerque and M. G. Cottam (eds.), *Polaritons in Periodic and Quasiperiodic Structures* (Elsevier, Amsterdam, 2004).
22. E. Maciá, *Rep. Prog. Phys.* **69**, 397 (2006).
23. E. Braun, Y. Eichen, U. Sivan and G. Ben-Yoseph, *Nature* **391**, 775 (1998).
24. C. Treadway, M. G. Hill and J. K. Barton, *Chem. Phys.* **281**, 409 (2002).
25. P. Carpena, P. B Galván, P. Ch. Ivanov and H. E. Stanley, *Nature* **418**, 955 (2002); **421**, 764 (2003).
26. F. A. B. F. de Moura, M. L. Lyra and E. L. Albuquerque, *J. Phys.: Condens. Matter* **20**, 075109 (2008).
27. D. Klotsa, R. A. Römer and M. S. Turner, *Biophys. J.* **89**, 2187 (2005).
28. G. Cuniberti, L. Craco, D. Porath and C. Dekker, *Phys. Rev. B* **65**, 241314(R) (2002).
29. R. G. Sarmento, E. L. Albuquerque, P. D. Session Jr., U. L. Fulco and B. P. W. de Oliveira, *Phys. Lett. A* **373**, 1486 (2009).
30. H. Sugiyama and I. Saito, *J. Am. Chem. Soc.* **118**, 7063 (1996).
31. A. A. Voityuk *et al.*, *J. Chem. Phys.* **114**, 5614 (2001).
32. H. Zhang *et al.*, *J. Chem. Phys.* **117**, 4578 (2002).
33. Y. A. Berlin, A. L. Burin and M. A. Ratner, *J. Am. Chem. Soc.* **123**, 260 (2001); *Chem. Phys.* **275**, 61 (2002).
34. E. Maciá, *Phys. Rev. B* **74**, 245105 (2006).
35. E. Maciá, F. Triozon and S. Roche, *Phys. Rev. B* **71**, 113106 (2005).
36. J. Ladik, A. Bende and F. Bogár, *J. Chem. Phys.* **128**, 105101 (2008).
37. I. Dunham *et al.*, *Nature* **402**, 489 (1999).
38. F. Axel, J. P. Allouche and Z. Y. Wen., *J. Phys.: Condens. Matter* **4**, 8713 (1992).
39. E. L. Albuquerque and M. G. Cottam, *Phys. Rep.* **376**, 225 (2003).
40. M. Dulea, M. Johansson and R. Riklund, *Phys. Rev. B* **45**, 105 (1992); *Phys. Rev. B* **46**, 3296 (1992); *Phys. Rev. B* **47**, 8547 (1993).
41. H. Aynaou, V. R. Velasco, A. Nougaoui, E. H. El Boudouti, B. Djafari-Rouhani and D. Bria, *Surf. Sci.* **538**, 101 (2003).
42. R. G. Sarmento, G. A. Mendes, E. L. Albuquerque, U. L. Fulco, M. S. Vasconcelos, P. Ujsághy, V. N. Freire and E. W. S. Caetano, *Phys. Lett. A* **376**, 2413 (2012).
43. S. Roche, D. Bicout, E. Maciá and E. Kats, *Phys. Rev. Lett.* **91**, 228101 (2003); *Phys. Rev. Lett.* **92**, 109901(E) (2004).
44. F. A. B. F. de Moura and M. L. Lyra, *Phys. Rev. Lett.* **81**, 3735 (1998).
45. B. Kramer and A. MacKinnon, *Rep. Prog. Phys.* **56**, 1469 (1993); F. Domínguez-Adame, V. A. Malyshev, F. A. B. F. de Moura and M. L. Lyra, *Phys. Rev. Lett.* **91**, 197402 (2003); R. A. Romer and H. Schulz-Baldes, *Eu-*

rophys. Lett. **68**, 247 (2004).
46. E. Abrahams, P. W. Anderson, D. C. Licciardello and T. V. Ramakrishnan, *Phys. Rev. Lett.* **42**, 673 (1979).
47. D. H. Dunlap, H. L. Wu and P. W. Phillips, *Phys. Rev. Lett.* **65**, 88 (1990); H.-L. Wu and P. Phillips, *Phys. Rev.Lett.* **66**, 1366 (1991).
48. F. M. Izrailev and A. A. Krokhin, *Phys. Rev. Lett.* **82**, 4062 (1999).
49. M. L. Ndawana, R. A. Romer and M. Schreiber, *Europhys. Lett.* **68**, 678 (2004).
50. E. L. Albuquerque, M. S. Vasconcelos, M. L. Lyra and F. A. B. F. de Moura, *Phys. Rev. E* **71**, 021910 (2005).
51. E. L. Albuquerque, M. L. Lyra and F. A. B. F. de Moura, *Physica A* **370**, 625 (2006).
52. R. G. Sarmento, U. L. Fulco, E. L. Albuquerque, E. W. S. Caetano and V. N. Freire, *Phys. Lett. A* **375**, 3993 (2011).
53. A. Nitzan, *Annu. Rev. Phys. Chem.* **52**, 681 (2001).
54. M. Kohmoto, L. P. Kadanoff and C. Tang, *Phys. Rev. Lett.* **50**, 1870 (1983).
55. M. Hilke, *J. Phys. A* **30**, L367 (1997).
56. E. Lazo and M. E. Onell, *Phys. Lett. A* **283**, 376 (2001).
57. F. A. B. F. de Moura, M. N. B. Santos, U. L. Fulco, M. L. Lyra, E. Lazo and M. E. Onell, *Eur. Phys. J. B* **36**, 81 (2003).
58. M. Hilke, *Phys. Rev. Lett.* **91**, 226403 (2003).
59. H. Yamada, *Phys. Lett. A* **332**, 65 (2004).
60. B. L. Altshuler, *Jpn. J. Appl. Phys. Suppl.* **26**, 1938 (1987).
61. S. N. Evangelou, *Prog. Theor. Phys. Suppl. Jpn.* **116**, 319 (1994); S. N. Evangelou and P. Argyrakis, *Phys. Rev. B* **51**, 3489 (1995).
62. R. Landauer, *IBM J. Res. Dev.* **1**, 223 (1957); *Philos. Mag.* **21**, 863 (1970); *J. Math. Phys.* **37**, 223 (1996).
63. M. Buttiker, *Phys. Rev. B* **35**, 4123 (1987).
64. E. Maciá, *Nanotechnology* **16**, S254 (2005); *Nanotechnology* **17**, 3002 (2006).
65. L. M. Bezerril, D. A. Moreira, E. L. Albuquerque, U. L. Fulco, E. L. de Oliveira and J. S. de Sousa, *Phys. Lett. A* **373**, 3381 (2009).
66. M. S. Xu, S. Tsukamoto, S. Ishida, M. Kitamura, Y. Arakawa, R. G. Endres and M. Shimoda, *Appl. Phys. Lett.* **87**, 083902 (2005).
67. V. Mugica, M. Kemp, A. Roitberg and M. A. Ratner, *J. Chem. Phys.* **104**, 7296 (1996).
68. J. Chen, M. A. Reed, A. M. Rawlett and J. M. Tour, *Science* **286**, 1550 (1999); M. A. Reed, J. Chen, A. M. Rawlett, D. W. Price and J. M. Tour, *Appl. Phys. Lett.* **78**, 3735 (2001).
69. H. W. Fink and C. F. D. Schönenberger, *Nature* **398**, 407 (2005); F. D. Lewis, X. Y. Liu, J. Q. Liu, S. E. Miller, R. T. Hayes and M. R. Wasielewski, *Nature* **406**, 51 (2000); B. Giese, J. Amaudrut, A. K. Koëhler, M. Spormann and S. Wessely, *Nature* **412**, 318 (2001).
70. M. A. Stroscio and M. Dutta, *Biological Nanostructures and Applications of Nanostructures in Biology: Electrical, Mechanical & Optical Properties* (Kluwer, New York, 2004).
71. E. Maciá, *Rev. Adv. Mater. Sci.* **10**, 166 (2005).